

A comparison of bulk-sensitive spectroscopic probes of Yb valence in Kondo systems

L. Moreschini¹, C. Dallera², J.J. Joyce³, J.L. Sarrao³, E.D. Bauer³, V. Fritsch³, S. Bobev³, E. Carpena², G. Monaco⁴, G. Panaccione⁵, P. Lacovig⁵, G. Paolicelli⁶, A. Fondacaro⁶, P. Torelli⁷, and M. Gioni¹

¹ IPN, Ecole Polytechnique Fédérale (EPFL), CH-1015 Lausanne, Switzerland

² INFN-Dipartimento di Fisica, Politecnico di Milano, p. Leonardo da Vinci 32, 20133 Milano Italy

³ Los Alamos National Laboratory, Los Alamos, New Mexico 87545, USA

⁴ European Synchrotron Radiation Facility (ESRF), 38043 Grenoble Cédex, France

⁵ Laboratorio TASC, INFN, Area Science Park, S.S. 14, Km 163.5

⁶ INFN and Dipartimento di Fisica, Università di Roma III, I-00146 Roma, Italy

⁷ LURE, Université de Paris-Sud, F-91898 Orsay, France

(Dated: August 12, 2006)

We exploited complementary synchrotron radiation spectroscopies to study the Yb $4f$ electronic configuration in three representative intermediate-valence materials: YbAl₃, YbInCu₄, and YbCu₂Si₂. High-resolution x-ray absorption (PFY-XAS), resonant inelastic x-ray scattering (RIXS) and hard x-ray photoemission (HAXPES) data all show characteristic temperature-dependent changes of the Yb valence. For each material, the increments measured from low (20 K) to high (300 K) temperature by the different probes are quite similar. The estimated RIXS and XAS valences are consistently higher than the HAXPES values. We briefly discuss the possible origin of this discrepancy.

PACS numbers: 71.28.+d, 78.70.En, 78.70.Dm, 79.60.-i

High-energy spectroscopies like photoemission (PES) or x-ray absorption (XAS) provide unique insight in the dynamics of the $4f$ electrons that are at the origin of ‘Kondo’ phenomena in intermediate valence (IV) materials, like many Ce or Yb metallic compounds¹⁻³. The fractional occupancy n_f of these states reflects their hybridization with extended conduction band electrons. The Anderson Impurity Model (AIM), that embodies the minimal theoretical description of this phenomenon, predicts for n_f a simple dependence on hybridization and temperature⁴, via the single parameter (T/T_K). T_K is the material-dependent Kondo temperature. It grows exponentially with the $4f$ -band hybridization, and sets the low-energy scale of the problem. It is generally assumed that these generic features of the AIM survive in the more elaborate and applicable theoretical lattice schemes⁵.

Some aspects of a scaling behavior have been confirmed qualitatively by conventional XAS⁶⁻⁸ and core level PES⁹ in Ce and Yb IV compounds, and even quantitatively by more elaborate photon in - photon out experiments¹⁰. Scaling should be especially evident in valence band PES data, since the intensity of the Kondo resonance (KR), the characteristic many-body feature straddling the Fermi level^{4,11}, directly reflects the configuration mixing in the ground state. PES data, on the contrary, have been controversial, with results from cleaved single crystals^{12,13} failing to exhibit the T/T_K dependence generally observed in polycrystalline samples^{2,3,14,15}. The issue is confused by the short probing depth (5-10 Å) of low-energy PES, and by the tendency of the Yb (Ce) ions to adopt a surface electronic configuration different from that of the bulk. More recent soft¹⁶⁻²⁰ and hard x-ray PES (HAXPES)^{19,21} experiments with enhanced bulk sensitivity generally support a Kondo scenario interpretation.

The purpose of the present paper is to compare intrinsically bulk-sensitive photon in - photon out spectro-

scopies like XAS and resonant inelastic x-ray spectroscopy (RIXS) with HAXPES. We present data on three representative Yb IV compounds: YbAl₃, YbInCu₄, and YbCu₂Si₂. YbCu₂Si₂ and YbAl₃ are typical Kondo systems, with Kondo temperatures $T_K \sim 40-60$ K and, respectively, $T_K \sim 400$ K^{12,14}. YbInCu₄ exhibits at $T_V = 42$ K an isostructural first-order transition that affects the electronic and magnetic properties. The valence suddenly increases from 2.83 to 2.96 for $T > T_V$, while the Kondo temperature drops from $T_K \sim 400$ K ($T < T_V$) to $T_K \sim 20$ K ($T > T_V$)^{22,23}.

We show that the different spectroscopies agree on two major points. Firstly, they all indicate an increase of the Yb valence (at 20 K) from YbAl₃ to YbCu₂Si₂, in agreement with the known properties of the three compounds. Secondly, they reveal the expected increase of the Yb valence with temperature. The valence values extracted from the XAS/RIXS data are closer to the estimates from non spectroscopic measurements. Photoemission provides a more direct view of the Yb $4f$ states, but it remains, even at high energy, more sensitive to the sample preparation procedure. In our experiment, the perturbation produced by scraping the surface may well have extended over a thickness comparable to - and possibly larger than - the probing depth of HAXPES (~ 60 Å). We conclude that XAS/RIXS is the more consistent probe of the bulk Yb electronic configuration.

We have used flux-grown single crystals characterized by x-ray diffraction and magnetic susceptibility measurements. All measurements were performed at the undulator beamline ID16 of the ESRF (Grenoble) equipped with a Si(111) double crystal monochromator. For partial fluorescence yield XAS (PFY-XAS) and RIXS experiments, freshly scraped samples were mounted on a He cryostat and measured in high (10^{-8} mbar) vacuum. We used a Rowland circle spectrometer based on a spherically bent Si(620) crystal, and a Si avalanche pho-

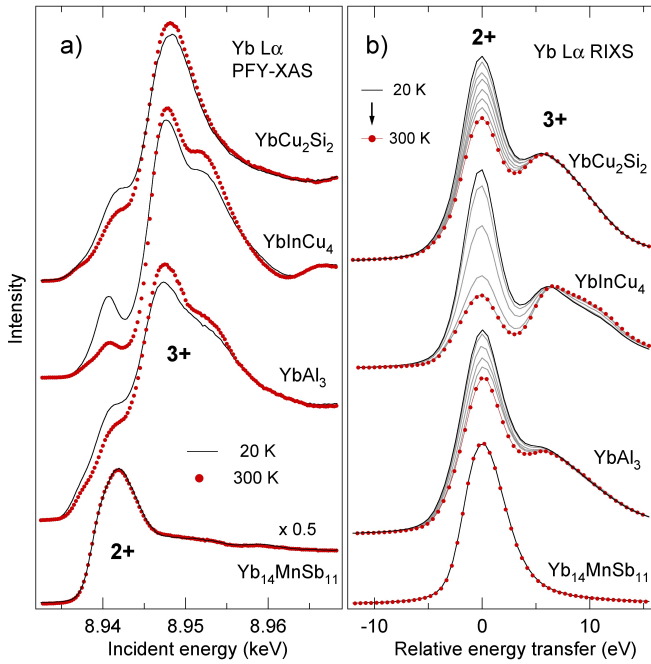


FIG. 1: a) PFY-XAS spectra of three IV compounds and of divalent Yb₁₄MnSb₁₁ at 20 K and 300 K. b) RIXS spectra measured between 20 K and 300 K, at $h\nu_{in}=8.941$ keV, the maximum of the Yb²⁺ resonance profile.

todiode detector. The total energy resolution was ~ 1.5 eV. For HAXPES the beamline was equipped with a Si(333) channel-cut post-monochromator working in near backscattering condition at $h\nu=5934$ eV. The samples were scraped by a diamond file at 10^{-9} mbar, and measured by the VOLPE electron spectrometer²⁴. The combined (photons + electrons) energy resolution now attainable by this instrument is $\Delta E \sim 70$ meV, but for the present experiment we used a lower resolution $\Delta E \sim 0.25$ eV in a trade-off for intensity.

The PFY-XAS and RIXS results for the IV materials and for the divalent reference compound Yb₁₄MnSb₁₁ are summarized in Fig. 1. The Yb L_3 PFY-XAS spectra measure, as a function of the incident photon energy, the intensity of the $L\alpha_1$ ($3d \rightarrow 2p$) fluorescence ($h\nu_0=7415$ eV) emitted after the creation of an Yb $2p$ hole: $2p^6 4f^N \rightarrow 2p^5 4f^N \epsilon d \rightarrow 2p^6 3d^9 4f^N$. The intrinsic spectral line width is set by the shallower $3d$ hole ($\Delta E \sim 0.6$ eV), rather than by the deep $2p$ hole ($\Delta E \sim 5.3$ eV) as in conventional XAS. PFY-XAS is not strictly equivalent to XAS with a reduced line width, but it gives access to finer spectral details^{25–27}. The Yb $L\alpha$ RIXS spectra reproduce, for a given $h\nu_{in}$, the energy distribution of the photons emitted in the same de-excitation channel. The energy transfer ($h\nu_{in} - h\nu_{out}$) is the energy difference between the excited final state and the ground state.

In Yb IV materials, L_3 (PFY-)XAS is a superposition of absorption spectra from the Yb²⁺ and Yb³⁺ components of the hybrid ground state. The intensities of each contribution for our analysis is assumed proportional to the weight of the corresponding initial state configurations⁸. The spectra of Fig.

1a exhibit prominent Yb³⁺ features at 8948 eV, and smaller Yb²⁺ signals at ~ 7 eV lower energy. Spectral weight is transferred from the 2+ to the 3+ component at the higher temperature in all the IV systems, following the increase of the Yb valence predicted by a Kondo scenario^{4,10}.

The RIXS spectra similarly exhibit Yb²⁺ and Yb³⁺ components, which can be selectively enhanced by an appropriate choice of the incident photon energy. The spectra of Fig. 1b correspond to the maximum of the Yb²⁺XAS (and RIXS) signal. This is a favorable condition because small valence changes have a larger effect on the minority Yb²⁺ weight. Changes in the Yb²⁺ intensity reflect corresponding *relative* changes of the Yb²⁺ weight in the initial state. Knowledge of the Yb valence at e.g. 300 K, either from the XAS spectrum, or by a combined analysis of the Yb²⁺ and Yb³⁺ resonance profiles²⁷, yields the valence $v(T)$ at all temperatures. For YbAl₃ and YbInCu₄ we also performed continuous measurements of the Yb²⁺ RIXS intensity at a rate of ~ 1 K/minute. $v(T)$ (Fig. 4) follows a smooth ‘Kondo’ dependence in YbAl₃, and the overall valence increase is $\Delta v=0.05$. In YbInCu₄ the Yb valence exhibits a jump at $T_V=42$ K, and no further evolution above T_V , as expected from $T_K \sim 20$ K in the high-temperature phase. $v(T)$ does not saturate to the low-T value immediately below T_V , in contrast to the electrical resistivity or the magnetic susceptibility²³. The further low-T evolution suggests a distribution of T_V ’s, possibly associated with disorder induced by scraping, and extending over a distance comparable with the probing depth of RIXS ($\gg 100$ Å). This is much larger than the thickness of a proposed perturbed region under a cleaved surface, as estimated by PES²⁰. Nonetheless, the RIXS data of Fig. 4 is clear spectroscopic evidence of a first-order-like transition at T_V .

The valence band (VB) and Yb 3d core level HAXPES results are shown in Fig. 2 and Fig. 3, after the usual subtraction of inelastic Shirley backgrounds. The VB spectra exhibit the typical features of IV Yb compounds: the spin-orbit-split Yb²⁺ KR near E_F , and an Yb³⁺ multiplet at 5-12 eV. Peaks at ~ 4 eV in YbInCu₄ and YbCu₂Si₂ are from Cu $3d$ states. At this photon energy ($h\nu=5935$ eV) the contribution from the topmost surface layer is small ($\sim 5\%$)²⁸, and the spectra are free from the broad surface signal typical of low-energy PES. The Yb³⁺ intensity in YbInCu₄ is somewhat smaller than in published HAXPES data²¹. The (Yb²⁺/Yb³⁺) intensity ratio at 300 K is largest for YbAl₃ and smallest for YbInCu₄, and in all compounds the intensity of the divalent doublet decreases at high temperature, with a corresponding growth of the Yb³⁺ multiplet. Notice that the simple thermal broadening of the Fermi edge would not affect the integrated intensity of a band feature. The VB HAXPES results are therefore consistent with the RIXS data of Fig. 1, and with a Kondo scenario.

The Yb valence can be estimated from the Yb²⁺ and Yb³⁺+VB PES intensities as: $v=2 + 14 \cdot I(3+)/[14 \cdot I(3+)+13 \cdot I(2+)]$. We have isolated the $4f$ signal in YbInCu₄ by comparison with the spectrum of LuInCu₄, shown in Fig. 2 after removing the atomic-like Lu $4f$ doublet centered at ~ 8 eV. Integrating the difference spectrum over 2+ and 3+ energy windows, yields $v(20$ K) $=2.65 \pm 0.03$ and $v(300$ K) $=2.77 \pm 0.03$. For YbAl₃ and

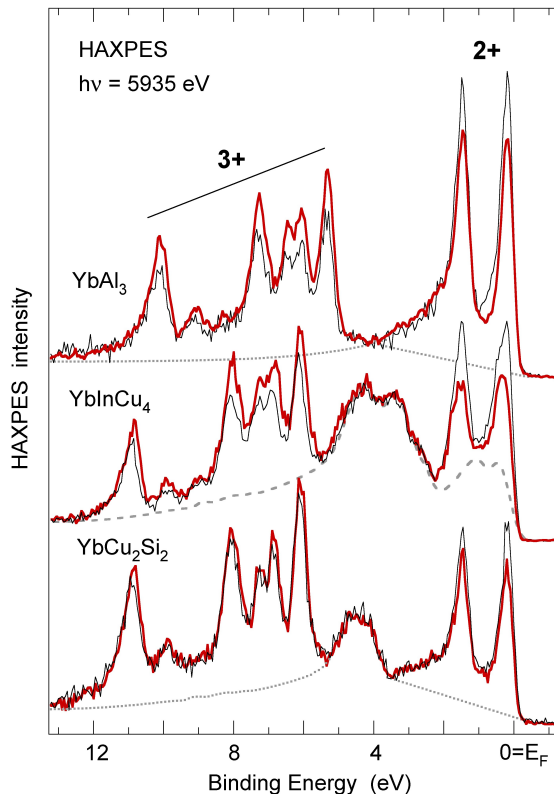


FIG. 2: HAXPES ($h\nu=5935$ eV) valence band spectra measured at 20 K (thin solid lines) and 300 K (thick (red) solid lines). The dashed line is the spectrum of LuInCu_4 , after subtraction of the atomic-like $4f$ doublet. The dotted lines are phenomenological non- $4f$ backgrounds (see text).

YbCu_2Si_2 the corresponding Lu compounds could not be measured, and we used information from published soft x-ray VB spectra¹². Assuming, as a first approximation, the same photon energy dependences for the $4f/(\text{non-}4f)$ intensity ratio as in YbInCu_4 , yields the values reported in Fig. 4. In both cases the correction from the non- $4f$ states is small ($\Delta v \sim 0.06$). Subtracting phenomenological backgrounds from the spectra (dotted lines), yields similar results. The error bars are large but acceptable, since our goal is to compare the different probes, rather than to determine the Yb valence with high accuracy.

The $3d$ core levels are good indicators of the electronic configuration in $4f$ materials. The Yb $3d$ lines are too deep for standard Al $K\alpha$ sources, but can be reached by HAXPES. The $j=3/2$ and $j=5/2$ spin-orbit-split manifolds, separated by ~ 50 eV, are further split into a sharp $3d^9 4f^{14}$ (Yb^{2+}) final state and a $3d^9 4f^{13}$ (Yb^{3+}) multiplet (Fig. 3). Broad plasmon features are observed ~ 25 eV below the leading peak²¹. YbAl_3 also exhibits, besides plasmon replicas, a very intense Al $1s$ peak, with an associated strong satellite. We have determined the Yb valence by integrating the intensity of the $j=5/2$ manifolds within separate $2+$ and $3+$ energy windows. The contribution of the overlapping plasmon satellite in YbAl_3 was removed by subtracting a scaled replica of the

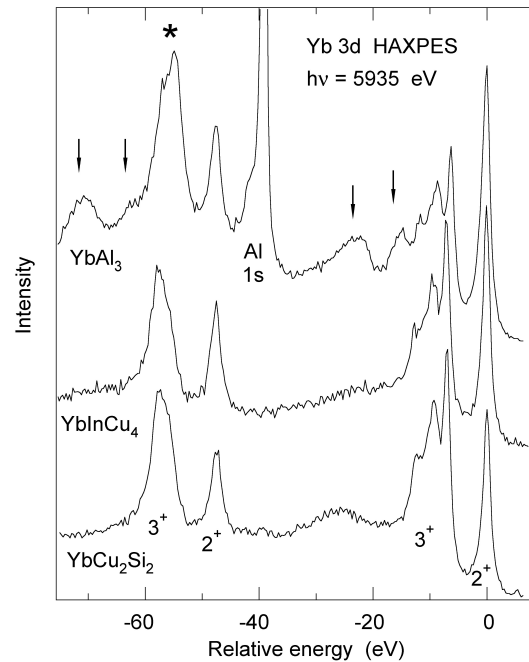


FIG. 3: Low-temperature spectra of the Yb $3d$ core levels. Each spin-orbit manifold is split into $2+$ and $3+$ components. The arrows mark strong plasmon satellites in YbAl_3 . The asterisk marks a plasmon replica of the strong Al $1s$ peak.

$3+$ line shape, from the YbCu_2Si_2 spectrum.

The experimental results are summarized in Fig. 4. The RIXS valence is always largest, and consistent with previous XAS data (Table I). The agreement with thermodynamic and magnetic measurements is rather good. As already noted, the RIXS temperature dependence displays, as expected, a smooth variation in YbAl_3 and a step at T_V in YbInCu_4 . As to photoemission, there is a considerable scattering in the literature (Table I), with low-energy PES results showing lower valences than soft- and hard x-ray PES. Our core level results are consistent with the latter, and smaller by 0.05 to 0.1 than the RIXS values. The data points are too sparse to confirm the sharp jump in YbInCu_4 , suggested by Ref. 21. At present, the low signal forbids a continuous T-dependent HAXPES measurement.

The VB spectra yield consistently lower values than the $3d$ core data. In YbAl_3 it may point to an inadequate background removal procedure. This problem is especially delicate in HAXPES. For instance, the $\text{Yb}(4f)/\text{Al}(3s)$ atomic cross sections ratio decreases by one order of magnitude between 1000 eV and 6000 eV²⁹. A comparison with Lu or La sister compounds would therefore be desirable. The difference is smaller for YbCu_2Si_2 and YbInCu_4 . In the latter the valence transition is smeared over 50 K, which again suggests the possible shortcomings of scraping the surface for HAXPES. Remarkably, the measured relative valence changes are quite similar for all techniques. This suggests further systematic studies of the origin of the discrepancies, namely varying the photon energy (probing depth) and comparing data from

TABLE I: Estimated Yb valence from high-energy spectroscopies

	YbAl ₃	YbInCu ₄	YbCu ₂ Si ₂
PES ($h\nu \leq 120$ eV)	2.63 ¹²	2.57(20 K) - 2.86 (300 K) ²⁰	2.63 ¹²
PES ($h\nu \geq 500$ eV)	2.77 (10 K) ¹⁴ ; 2.65 (20 K) ¹⁹	2.67(20 K) - 2.83 (300 K) ^{18,20} 2.60(20 K) - 2.72 (70 K) ³⁰	
Core level HAXPES	2.71 (180 K) ¹⁹	2.74(10 K) - 2.90 (220 K) ²¹	
XAS	2.78 (20 K) - 2.83 (300 K) ⁸	2.83(20 K) - 2.96 (300 K) ³¹	2.82(20 K) - 2.89 (300 K) ⁸

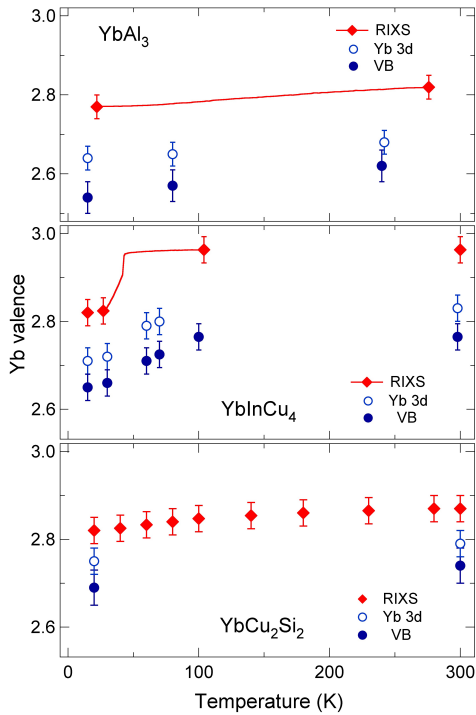


FIG. 4: Summary of the valence values determined by the various spectroscopies. The solid lines refer to continuous temperature-dependent RIXS measurements.

scraped and cleaved samples. From the theoretical side, first principles calculations of the PES and XAS spectra, including dynamical effects³², would reduce the uncertainties of the present analysis, and could reveal possible systematic differences between the two spectroscopic probes.

In summary, we have presented a comparison of photon in - photon out and high-energy PES results in three representative IV materials. The data generally display a temperature and T_K dependence consistent with a Kondo scenario, and quite similar values for the relative valence changes. They also show quantitative differences. RIXS and high-resolution PFY-XAS show n_f values more consistent with thermodynamic models. HAXPES, albeit not totally free from the influence of surface disorder and surface preparation techniques, is much more bulk sensitive than standard PES, and provides a unique and direct view of the $4f$ many-body spectral features.

We gratefully acknowledge the expert support of the ESRF staff. The HAXPES electron spectrometer has been developed by the VOLPE collaboration²⁴ and supported by the EU under Contract HPRI-CT-2001-50032 and by the Swiss National Science Foundation. LANL support was provided by the US-DOE under OBES.

¹ A.C. Hewson, *The Kondo Problem to Heavy Fermions*, (Cambridge University Press, 1993).
² Allen *et al.*, *Adv. Phys.* **35**, 275 (1986).
³ D. Malterre, M. Grioni, and Y. Baer, *Adv. Phys.* **45**, 299 (1996).
⁴ N.E. Bickers, D.L. Cox, and J.W. Wilkins, *Phys. Rev. B* **36**, 2036 (1987).
⁵ A.N. Tahvildar-Zadeh, M. Jarrel, and J.K. Freericks, *Phys. Rev. Lett.* **80**, 5168 (1998).
⁶ J. Röhler, *J. Magn. Magn. Mat.* **47-48**, 175 (1985).
⁷ E. Beaurepaire, J.P. Kappler, and G. Krill, *Solid State Commun.* **57**, 145 (1986).
⁸ J.M. Lawrence, G.H. Kwei, P.C. Canfield, J.G. DeWitt, and A.C. Lawson, *Phys. Rev. B* **49**, 1627 (1994).
⁹ J.C. Fuggle *et al.*, *Phys. Rev. B* **27**, 7330 (1983).
¹⁰ C. Dallera *et al.*, *Phys. Rev. Lett.* **88**, 196403 (2002).

¹¹ O. Gunnarsson and K. Schönhammer, *Phys. Rev.* **28**, 4315 (1983).
¹² J.J. Joyce *et al.*, *Phys. Rev.* **54**, 17515 (1996).
¹³ J.J. Joyce, A.J. Arko, L.A. Morales, J.L. Sarrao, and H. Höchst, *Phys. Rev.* **63**, 197101 (2001).
¹⁴ L.-H. Tjeng *et al.*, *Phys. Rev. Lett.* **71**, 1419 (1993).
¹⁵ P. Weibel *et al.*, *Z. Phys. B* **91**, 337 (1193).
¹⁶ E. Weschke *et al.*, *Phys. Rev. B* **44**, 8304 (1991).
¹⁷ A. Sekiyama *et al.*, *Nature (London)* **403**, 396 (2000).
¹⁸ H. Sato *et al.*, *Phys. Rev. B* **69**, 165110 (2004).
¹⁹ S. Suga *et al.*, *J. Phys. Soc. Jpn* **74**, 2880 (2005).
²⁰ S. Schmidt, S. Hüfner, F. Reinert, and W. Assmus, *Phys. Rev. B* **71**, 195110 (2005).
²¹ H. Sato *et al.*, *Phys. Rev. Lett.* **93**, 246404 (2004).
²² Felner and I. Nowik, *Phys. Rev. B* **33**, 617 (1986).
²³ J.L. Sarrao *et al.*, *Phys. Rev. B* **54**, 12207 (1996).

- ²⁴ P. Torelli *et al.*, Rev. Sci. Instrum. **76**, 023909 (2005).
- ²⁵ K. Hämäläinen, D.P. Siddons, J.B. Hastings, and L.E. Berman, Phys. Rev. Lett. **67**, 2850 (1991).
- ²⁶ A. Kotani and S. Shin, Rev. Mod. Phys. **73**, 203 (2001).
- ²⁷ C. Dallera *et al.*, Phys. Rev. B **68**, 245114 (2003).
- ²⁸ M. Sacchi *et al.*, Phys. Rev. B **71**, 155117 (2005).
- ²⁹ J.J. Yeh and I. Lindau, At. Data Nucl. Data Tables **32**, 1 (1985).
- ³⁰ D.P. Moore *et al.*, Phys. Rev. B **62**, 16492 (2000).
- ³¹ A.L. Cornelius *et al.*, Phys. Rev. B **56**, 7993 (1997).
- ³² O. Wessely, M.I. Katsnelson, and O. Eriksson, Phys. Rev. Lett. **94**, 167401 (2005).